Research Article

Journal of PeptideScience

Received: 26 February 2009 Revised: 19 June 2009 Accepted: 22 June 2009 Published online in Wiley Interscience: 18 August 2009

(www.interscience.com) DOI 10.1002/psc.1165

Membrane association and selectivity of the antimicrobial peptide NK-2: a molecular dynamics simulation study

Jutarat Pimthon,[a,b] Regine Willumeit,[c] Andreas Lendlein[a] and Dieter Hofmann[a]*

In an effort to better understand the initial mechanism of selectivity and membrane association of the synthetic antimicrobial peptide NK-2, we have applied molecular dynamics simulation techniques to elucidate the interaction of the peptide with the membrane interfaces. A homogeneous dipalmitoylphosphatidylglycerol (DPPG) and a homogeneous dipalmitoylphosphatidylethanolamine (DPPE) bilayers were taken as model systems for the cytoplasmic bacterial and human erythrocyte membranes, respectively. The results of our simulations on DPPG and DPPE model membranes in the gel phase show that the binding of the peptide, which is considerably stronger for the negatively charged DPPG lipid bilayer than for the zwitterionic DPPE, is mostly governed by electrostatic interactions between negatively charged residues in the membrane and positively charged residues in the peptide. In addition, a characteristic distribution of positively charged residues along the helix facilitates a peptide orientation parallel to the membrane interface. Once the peptides reside close to the membrane surface of DPPG with the more hydrophobic side chains embedded into the membrane interface, the peptide initially disturbs the respective bilayer integrity by a decrease of the order parameter of lipid acyl chain close to the head group region, and by a slightly decrease in bilayer thickness. We found that the peptide retains a high content of helical structure on the zwitterionic membrane-water interface, while the loss of α-helicity is observed within a peptide adsorbed onto negatively charged lipid membranes.

Supporting information may be found in the online version of this article

Keywords: MD simulations; peptide-lipid interaction; lipid bilayers; electrostatic; anionic; zwitterionic; surface binding

Introduction

Natural antimicrobial peptides (AMPs), important effectors in the innate immune system, and their synthetic analogs are currently being developed as potential new therapeutic agents to overcome the pathogenic bacterial resistance [1–3]. These compounds display a broad spectrum of activity against various bacteria, fungi, protozoa, enveloped viruses, malignant cells and parasites. The great advantage of some of these peptides is that they physically destroy cell membranes of mono-cellular (prokaryotic) organisms while being basically benign to cells of multicellular (eukaryotic) organisms such as humans [2,4]. In recent years, thousands of native and *de novo* designed AMPs have become available (cf. AMSDb http://www.bbcm.univ.trieste.it/~tossi/pag1.htm). These peptides vary considerably in sequences, lengths, secondary structures and spectra of activities. A number of models attempt to explain their modes of action (for review, see [5,6]). To transfer the properties of AMPs into application as antibiotics, it is important to understand the interaction of these agents with cell membranes and to identify – if possible – the particular region of such a peptide responsible for its selectivity against target microbes.

It is well established that the primary target site of action of AMPs is the outer leaflet of the bacterial cytoplasm membrane without the exploitation of a specific receptor [2]. Furthermore, by virtue of the AMP's net positive charge, the electrostatic interaction is likely to play an important role resulting in a selectivity towards negatively charged bacterial membranes and reducing the toxicity towards zwitterionic ones, i.e. overall neutral mammalian plasma membranes [1,4]. Many AMPs appear to disrupt a membrane via a common general mechanism, the 'carpet-like' model [7], in which the peptides bind parallel to the phospholipid head groups of the target membrane via electrostatic interaction leading to a carpet-like coverage of the respective membrane surface. After a critical local threshold concentration is reached, the peptides cause membrane permeation by means of the formation of toroidal transient holes in the membrane or via detergent-like action [5].

Andrä *et al*. [8] have designed and synthesized a 27 amino acid residues antibacterial peptide, termed NK-2, corresponding to the third and fourth helices (residues 39–65) of NK-lysin. This peptide differs by three amino acid positions from the parental copy (NH_3^+-Lys(K)^1-Ile(I)^2-Leu(L)^3-Arg(R)^4-Gly(G)^5-Val(V)^6-Cys(C)^7-Lys(K)^8-Lys(K)^9-Ile(I)^{10}-Met(M)^{11}-Arg(R)^{12}-Thr(T)^{13}-

* *Correspondence to: Dieter Hofmann, Institute of Polymer Research, GKSS Research Center, Kantstr. 55, D-14513 Teltow, Germany. E-mail: dieter.hofmann@gkss.de*

a *Institute of Polymer Research, GKSS Research Center, Kantstr. 55, D-14513 Teltow, Germany*

b *Department of Pharmaceutical Chemistry, Faculty of Pharmacy, Mahidol University, 447 Sri-Ayudhya Road, Bangkok 10400, Thailand*

c *Institute of Materials Research, GKSS Research Center, Max-Planck-Str., D-21502 Geesthacht, Germany*

Journal of PeptideScience

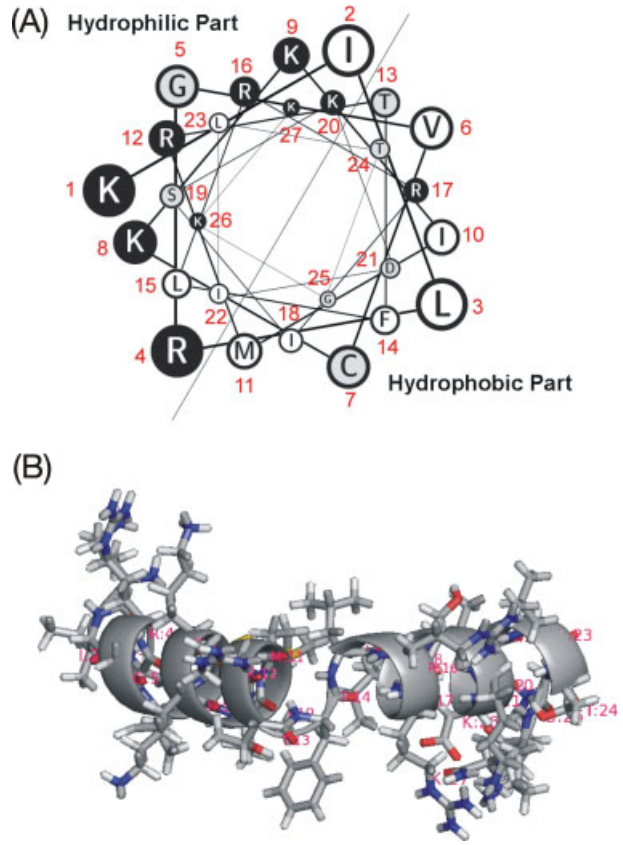

Figure 1. Helical wheel diagram and the secondary structure of NK-2 (A). Positively charged residues are presented as black filled circles, residual hydrophilic residues as grey shaded circles and hydrophobic residues as open circles. The line divides the helix into hydrophobic and hydrophilic parts. The assumed alpha helical structure of NK-2 (B) as taken from 1NKL.pdb [9] is in solid ribbon representation (grey) and amino acids are in stick representation: carbon (dark grey), hydrogen (light grey), nitrogen (blue), oxygen (red) and sulfur (yellow).

Phe(F)^{14}-Leu(L)^{15}-Arg(R)^{16}-Arg(R)^{17}-Ile(I)^{18}-Ser(S)^{19}-Lys(K)^{20}-Asp(D)^{21}-Ile(I)^{22}-Leu(L)^{23}-Thr(T)^{24}-Gly(G)^{25}-Lys(K)^{26}-Lys(K)^{27}-NH_2) and has an overall net positive charge (+10). Derived from the NMR-structure of NK-lysin [9], it is assumed that NK-2 has an amphipatic a helix–hinge–helix structure (Figure 1(A) and (B)), resembling the structure of cecropin A [10]. The attractive features of NK-2 as potential origin of a new class of peptide-based antibiotic drugs include its potent broad spectrum activity coupled with low hemolytic activity and no evidence of a mentionable cytotoxicity against human skin cells [8,10,11]. Besides its antimicrobial property, NK-2 is able to interact with some cancer cells lines with increased surface levels of negatively charged phosphatidylserine and subsequently causing membrane destruction [12].

In the past years, different experimental approaches have been employed to investigate the interaction of NK-2 with a wide range of model membranes [13,14]. Infrared reflection absorption spectroscopy (IRRAS) studies in combination with circular dichroism measurements indicated that the peptide is unstructured in aqueous solution, but adopts a high percentage of α-helical structure in membrane-like environment [8]. The long axis of the helix is oriented horizontally to the interface, as determined from the comparison between angle-dependent experimental IRRA spectra and simulated ones [14]. Small angle X-ray scattering (SAXS) experiments indicated the interaction between NK-2 and negatively charged palmitoyl-oleoyl-phosphatidylglycerol (POPG) vesicles resulting in bilayers of decreasing thickness [13]. Using specular X-ray reflectivity studies as well as IRRAS measurements, the results revealed that NK-2 adsorbs and inserts into condensed (gel) and fluid phase of negatively charged phosphatidylglycerol (PG) monolayers even at high surface pressure. Adsorption of NK-2 onto condensed dipalmitoylphoshatidylglycerol (DPPG) monolayers leads to a fluidization of the aliphatic chains (increased transition pressure) [15]. Under similar experimental conditions, there is almost no interaction of NK-2 with condensed zwitterionic dipalmitoylphosphatidyl ethanolamine (DPPE) monolayers, only a very small portion is penetrating at low lateral pressure. In the case of the fluid palmitoyloleoylphosphatidylethanolamine (POPE) monolayer, penetration of NK-2 into membrane is observed at the low pressure that is squeezed out and only a small amount is still adsorbed at the lipid layer at high pressure [15]. With SAXS measurements on lipid bilayers, it was shown that NK-2 had no influence on the lamellar repeat distance of zwitterionic phosphatidylcholine (PC) liposomes but it induces a strong change of the inverse hexagonal phase transition temperature towards significant lower values for phosphatidylethanolamine (PE) liposomes [13]. Biosensor assays showed no mass increase on the interaction of NK-2 with zwitterionic palmitoyloleoylphosphatidylcholine (POPC) layers but detected association of the peptide with PE and PE/PG coated surfaces [10]. Although, according to experimental observations [8,13], the first step of the NK-2 membrane interaction resembles a carpet-like mechanism, the membrane-disrupting mechanism of NK-2 has remained uncertain. Detailed knowledge of the intra- and intermolecular interactions of the NK-2 peptide on the membrane – water interface is necessary to explain its complicated action exerted on membranes.

Molecular dynamics (MD) simulations have been used with great success to explore atomistic aspects of the interaction between peptides or proteins and various types of model cell membranes which are difficult to access experimentally [16–24]. Most of the simulations so far have looked into interactions between the respective peptide and liquid-expanded (fluid) lipid bilayers, the most relevant phase in biological membranes, which were in the case of eukaryotic cells mainly composed of neutral charge lipids like PCs. There are, however, some AMPs such as Gramicidin S [25], peptidyl-glycyl-leucine-carboxamide (PGLa) [26], aurein 1.2 [27], citropin 1.1 [27], maculatin 1.1 [27], a hybrid peptide of cecropin A and melittin [28], indolicidin [29], Clavanin A [30] and our peptide NK-2 [15] that showed the tendency also to penetrate into the gel state of (anionic) lipid bilayers before the gel to liquid-crystalline phase transition actually occurs and consequently affects the structural integrity of the membrane model. Besides, there is evidence that a relatively rigid membrane is required as an appropriate model for natural membranes when probing the peptide–lipid interaction [31]. Moreover, the gel phase is promoted in bacterial membranes when the AMPs interact with membrane interfaces [32,33]. Furthermore, AMPs caused a different perturbing effect on different phase states of model membranes. In addition, several lines of evidence suggest that the mechanism of action of AMPs is dependent on several parameters, such as lipid compositions and phase states of membrane lipids [29,34]. Therefore, investigating the interactions of AMPs with different thermodynamic states of the respective lipid membrane (gel or fluid phase) using MD to complement experimental methods is likely to provide deeper insight into possible membrane perturbations by AMPs.

In this study, we focus on the MD simulation of the NK-2 peptide–lipid association considering the liquid-condensed (gel)

phase of zwitterionic DPPE bilayers and anionic DPPG bilayers with one major aim being comparisons with previous experiments. Simulations regarding interactions of NK-2 with liquid-expanded (fluid) phases are in progress and will be published elsewhere [35]. One of the striking differences between PG and PE head groups is that PG has a net negative charge at physiological pH, whereas the zwitterionic PE carries no net charge. Hereby, to address the question on cell selectivity, DPPE and DPPG were chosen to mimic the lipid compositions of the human red blood cell membranes and bacterial cytoplasmic membranes (cf. [36,37] and references cited therein), respectively. Thus, the obtained results of this simulation will be useful for clarifying the cell selectivity and mechanisms for the action of AMPs. All simulations were run at a temperature of 303 K, at which DPPE (transition temperature [Tm] = 327.5 K) and DPPG (Tm = 314 K) bilayers exist in the gel phase.

The influence of different starting orientation of the peptide on the membrane binding characteristic is investigated. The study also addresses the question how the respective lipid-bilayer membranes modulate the structure of the peptide, as well as structure and dynamic of the respective membrane. The theoretical results are discussed in comparison with experiments and other theoretical calculations to shed light on the structure–activity relationships and to improve our understanding of mechanism of action of the AMP.

To our knowledge, there are no reported simulations of AMPs involving anionic DPPG and zwittrionic DPPE lipid bilayers in the gel state, widely used model membranes for experimentally studying the behavior of AMPs.

Methods

Computational Methods

All calculations and analyses were carried out with the CHARMM program [38] running on double core processors on an AMD Opteron cluster under Red Hat Enterprise Linux. The standard all-atom CHARMM-22 [39] program with the CMAP correction [40] and the CHARMM-27 [41] force field were used for peptide and lipids, respectively, and water was modeled by TIP3P [42,43]. The SHAKE algorithm [44] was used to keep the water molecules rigid throughout the simulation. The leap-frog algorithm was utilized in all simulations with a 1 femtosecond (fs) time step for the NK-2/lipid systems and 2 fs time step for NK-2/water system, respectively. The nonbonded and image atom lists were updated heuristically using a cutoff distance of 12 Å and 14 Å for the peptide in water and for the peptide–lipid system, respectively, and a relative dielectric constant of 1 was applied. The Lennard-Jones interactions were smoothed by using an atom-based force-switch method over 12–14 Å for the peptide–lipid system, and 10–12 Å for the peptide in water. Periodic boundary conditions were applied in all three dimensions and the long-range electrostatic interactions were handled by the particle mesh Ewald (PME) [45] algorithm using a sixth-order B-spline interpolation and a grid spacing of approximately 1 Å. To directly compare with in-house experiments, all simulations were performed at 303 K where the considered lipid bilayers are in the gel phase. The structure analysis for the NK-2/water system was carried out under the NPT (constant mole number, pressure and temperature) ensemble. The NK-2/lipid systems were performed in NPAT (constant normal pressure and lateral surface area of membranes and constant temperature) conditions and the NPγT (constant number of atoms, pressure, surface tension and temperature) ensemble, where the area per lipid is allowed to adjust during the insertion of the peptide into the membrane [46]. Although, we did not expect a significantly different behavior for the interfacial interaction at the liquid condensed phase system in NPAT and NPγT ensembles. The NPγT ensemble was utilized to avoid a possible artifact, i.e. membrane thinning, when the lipid bilayer begins to accommodate the peptide in the simulations performed on the NPAT ensemble. In addition, it was shown that it is necessary to incorporate a defined surface tension into a MD simulation to avoid long-wavelength undulations for the microscopic membrane patch [47]. However, γ is not exactly known for the simulated heterogeneous systems and a surface tension = 0 (being equivalent to NPT) would lead to compression of the system with the current CHARMM lipid parameters [48,49]. We therefore estimated γ based on the value that we had to apply to obtain reasonable properties of pure bilayer simulations [50]. However, a simulation with a correctly parameterized constant surface area with the NPAT ensemble can be directly comparable to an applied appropriate constant surface tension [18,51–53] With this in mind, the dynamics were performed under both the NPAT condition and NPγT with the above-mentioned value. In the present study, no significant differences in the critical results were found from the use of different ensembles (see Results and Discussion). Here, we observed a change in area per lipid between NPAT and NPγT of around 2% (from ~48.68 to 50.02 Å^2 in PG model and from 43.36 to 42.44 Å^2) over the course of simulation. An overview of the simulations performed is given in Table 1. A pressure of 1 atm was maintained by means of the Nosé-Hoover Langevin Piston algorithm [54] and the temperature was controlled by a Nosé-Hoover thermostat [55,56]. Atomic positions were saved every 0.5 ps for later analysis.

Table 1. Overview of simulations performed

Label	Systems[a]	Ensenble	Length of MD
PG1	NK-2_2/DPPG$_{224}$/water$_{10421}$/Na^+_{236}/Cl^-_{32}/	NPAT	29 ns
PG2	NK-2_2/DPPG$_{224}$/water$_{10421}$/Na^+_{236}/Cl^-_{32}/	NPγT(γ = 30)	29 ns
PE1	NK-2_2/DPPE$_{224}$/water$_{9704}$/Na^+_{30}/Cl^-_{50}/	NPAT	29 ns
PE2	NK-2_2/DPPE$_{224}$/water$_{9704}$/Na^+_{30}/Cl^-_{50}/	NPγT(γ = 10)	29 ns
NK	NK-2_1/water$_{7807}$/Na^+_{22}/Cl^-_{32}/	NPT	50 ns

DPPG, dipalmitoylphosphatidylglycerol; DPPE, dipalmitoylphosphatidyl-ethanolamine; PE, phosphatidylethanolamine; PG, phosphatidylglycerol; NPT, constant mole number, pressure and temperature; NPAT, constant normal pressure and lateral surface area of membranes and constant temperature; NPγT, constant number of atoms, pressure, surface tension and temperature.
[a] Subscripts correspond to the number of peptide or lipid or water molecules and Na^+ and Cl^- counterions in the system.

Journal of PeptideScience

Secondary structure assignments were made using the define secondary structure of proteins (DSSP) implemented in program SIMULAID [57]. Molecular graphics were created using Pymol [58], except the cluster analysis was done by visual molecular dynamics (VMD) [59]. Please note that we started the calculations in each case from a pre-equilibrated lipid bilayer in contact with a pure water phase as described in Ref. 50. This reference also contains an extensive consideration of the status of equilibration of the model. There, the simulated results were in good agreement with the values obtained from experiments. In the current study where these lipid bilayers were brought in contact with NK-2 molecules, only some basic parameters were considered to prove the equilibration of the system (cf. Table 1). For the lipid bilayers, we have monitored the area/lipid in the case of the performed NPγT ensemble simulations. There, we observed a fairly stable value of the area/lipid during the entire simulation time (data not shown), thus proving that the system is equilibrated. Please note that in the case of the simulation under NPAT ensemble, the area per lipid of the pre-equilibrated (starting) lipid bilayer was fairly close to the reported experiment data. In both NPAT and NPγT ensemble, we in addition also monitored the energy, temperature and pressure of the system (data not shown). The observed convergence of these properties is a further indication for the system equilibration.

Model Description

The aims of this study are to get insights into the conformational stability of the peptide NK-2 at anionic and zwitterionic lipid bilayer–water interfaces and its effect on the structure of model lipid systems during the initial approach from an aqueous phase. The study started with simple hydrated lipid bilayers of either anionic DPPG or zwitterionic DPPE. A more detailed description of these models is published elsewhere [50]. For comparison, a peptide simulation in water was also conducted.

Simulation of NK-2 in water

Since there are no available NMR or the X-ray crystallography for the peptide NK-2, the initial structure of the peptide NK-2 was taken by cutting residue 39–65 (the third and the fourth helical domains) from the NMR structures of NK-lysin (pdb-code 1NKL) [9], assuming that the substitution of three amino acids (see Section on Methods) and the depletion of the rest of the NK-lysin molecules did not affect the secondary structure of the peptide. The three necessary amino acid substitutions [8] in the native NK-lysin were performed manually using the builder module of the InsightII program, version 97.0 (Accelrys Inc., San Diego). The backbone and side chain torsion angles of the original residues were retained. The amino and carboxyl terminus was protonated and amidated, respectively. Subsequently, the peptide NK-2 was immersed in the middle of a pre-equilibrated 62.23 Å/edge cubic box of water where all water molecules were removed whose oxygen was within 2.6 Å from any atom of the peptide. To ensure an overall electrically neutral system close to the physiological ionic strength, 22 sodium and 32 chloride ions were randomly added. The entire system, which consists of 23 970 atoms, was briefly minimized using Steepest descend (SD) and adopted basis Newton-Raphson (ABNR) to eliminate bad van der Waals contacts. Following the energy minimization, the system was slowly heated to 303 K using increments of 10 K every 1000 steps and was allowed to equilibrate at this temperature for 70 ps. During this process, the velocity components were first assigned using a Gaussian distribution and then reassigned every 500 steps to keep the temperature at 303 $\pm$ 5 K. Following this stage, the system was equilibrated via MD simulation in the NPT ensemble for 50 ns. The temperature of the system was maintained via the Hoover thermostat with a thermostat coupling constant of 10 000 kcal mol^{-1} ps^{-2}, and a pressure of 1 atm was maintained via a Nose-Hoover Langevin piston barostat with a piston mass of 2000 atomic mass units and a collision frequency of 20 ps^{-1}.

Simulation of NK-2/DPPG system

The initial unit cell configuration of the NK-2/DPPG bilayer was prepared through several steps: (i) The pure DPPG bilayer consisting of 224 DPPG lipids (112 per leaflet) was taken from the pre-equilibrated configuration of our previous simulation. The details concerning the pure bilayer model construction, including its structural and dynamical properties, can be found in Pimthon *et al*. [50]. Thereafter, the water and counter-ions were completely removed from the pure bilayer model and the bilayer was then centered in a rectangular box of dimension 7.38 $\times$ 7.38 $\times$ 11.0 nm, with the bilayer surface oriented parallel to the *z* axis. (ii) The initial internal coordinates of the peptide were the same as those used at the start of the peptide simulation in water. Subsequently, the peptide was oriented parallel to the interface with its long axis parallel to the bilayer surface. To eliminate possible conformation bias and to increase the population of the starting configuration in the same simulation, two different peptide starting geometries, one with its hydrophobic face towards the membrane surface (CONF1, Figure 2(A) pink color) and the other with its hydrophilic face towards the interface (CONF2, Figure 2(A) violet color) were selected. These orientation situations were designed on the basis of the amphipathic nature of the peptide (cf. helical wheel diagram of NK-2 shown in Figure 1), in which hydrophilic and hydrophobic residues are preferentially found on opposite sides of the α-helix. A similar approach has been used by Larson and coworker [60] in an attempt to study the binding of an AMP on a POPC bilayer. This strategy is helpful to examine the influence of different initial configurations on the membrane-association process at the same simulation time. The centre of mass of the peptides was considered to be located 8 Å away from the respective surface of the bilayer (Figure 2(A)). This choice of distance is somewhat arbitrary but it is close enough that the early stages of membrane association can be examined within the length of our simulation. (iii) An equilibrated box of TIP3P waters with the same surface area as that of the bilayer was placed to create two slabs, one above and one below the bilayer, starting from the average carbonyl position of each leaflet and extending outwards, away from the center of the system, $z = 0$. Water molecules that overlapped lipid and peptide atoms within 2.2 Å or were outside the $z \pm 55$ Å dimensions of the unit cell were removed. To achieve a neutral charge system and to mimic a physiological ionic strength, 236 sodium and 32 chloride ions were added by randomly replacing an appropriate number of water molecules. The resulting system contained totally 60 073 atoms. The whole model was then subjected to a series of energy minimizations. First, the water and counter-ions were energy minimized for 200 steps of SD and 500 steps of ABNR algorithms during which the solute atoms were fixed. Second, only the peptide atoms were constrained with a force constant of 100 kcal mol^{-1} Å^{-2} in the beginning and then gradually decreasing to 50 and finally to

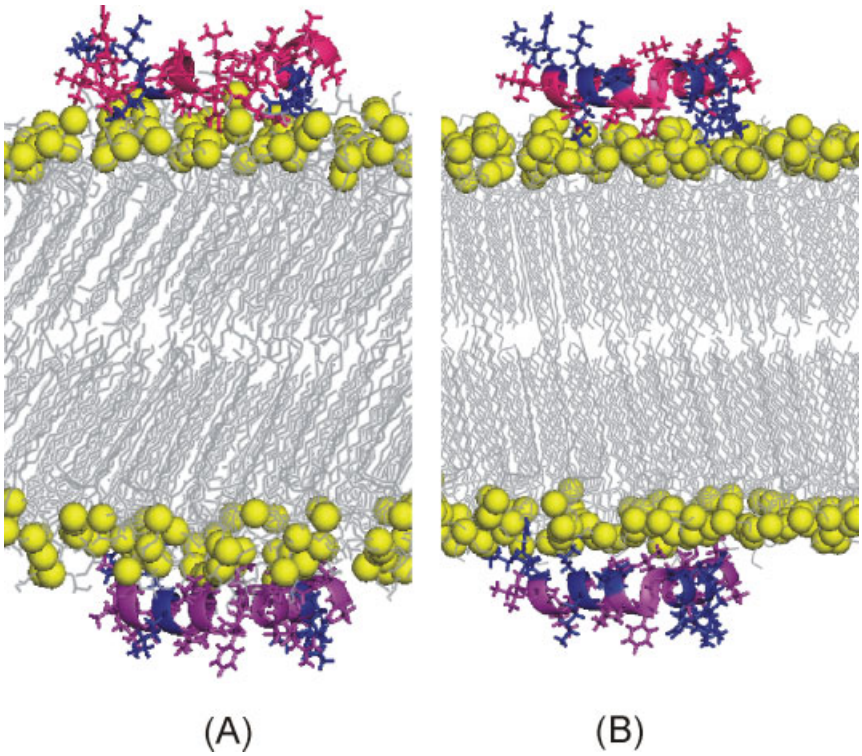

Figure 2. Snapshots of the initial configuration of (A) NK-2/DPPG and (b) NK-2/DPPE: The peptide with the hydrophobic side pointing towards membrane surface (CONF1) is colored in pink (top). The peptide with the hydrophobic side pointing outwards membrane surface (CONF2) is colored in violet (bottom). The lysine and arginine side chains are shown as blue sticks. Note that the water molecules and counter ions have been omitted for the sake of clarity.

10 kcal mol^{-1} Å^{-2}. At each step of the harmonic constrains, the system was energy minimized using 200 steps of the SD followed by 500 steps of ABNR. All residues were then again minimized with 200 steps of SD and 500 steps of ABNR without constraints. The resulting configurations were gradually heated from 103 K to 303 K over 10 ps, with atom velocities assigned from a Gaussian distribution every 500 integration steps. Afterwards, an additional MD equilibration was performed over a 90-ps period in which the velocity was reassigned only if the temperature of the system deviated more than 5 K from 303 K. (iv) The production run was performed by NPAT ensemble and by NPγT ensemble, where $\gamma = 30$ mN/m for 29 ns. The temperature of the system was maintained by a Nose-Hoover thermostat [55,56] with a coupling constant of 20 000 kcal mol^{-1}ps^{-2}, and the Nose-Hoover Langevin piston method [54] was used to keep a constant pressure of 1 atm with a piston mass of 3000 atomic mass units and a collision frequency of 10 ps^{-1}.

Simulation of NK-2/DPPE system

The protocol followed for the NK-2/DPPE system is basically the same as that used for the NK-2/DPPG system. This study was carried out in NPAT and NPγT ensemble, with $\gamma = 10$ mN/m, for 29 ns. The simulation system consisted of 224 DPPE molecules, 2 peptides (990 atoms), 30 chloride ions, 50 sodium ions and 9704 water molecules, resulting in 57 286 atoms in the unit cell size 6.97 × 6.97 × 11.5 nm. Details concerning construction and equilibration of pure DPPE bilayer can be found elsewhere [50]. The initial configuration of NK-2/DPPE system is shown in Figure 2(B).

Results and Discussion

NK-2 Structure in Water

The original NK-2 has a helix-hinge-helix structure, as it originates from the third and forth helices of the NK-lysin. Experimentally, it has been observed that in water, the peptide NK-2 exists predominantly in a largely unstructured conformation but folds into an α-helical secondary structure on binding to membrane-mimicking systems [8,14]. Our MD simulation of NK-2 in water, however, showed the peptide retains the helical structure throughout the molecule over the condition and duration of the present simulation study. This suggests that a bend, formed by Phe14 and Lys15, in the middle of the helix is slightly less stable. We did root mean square deviation calculations of C_α main chain and observed a stable profile after ~7 ns (Figure S1 as Supporting Information). This indicated it was not deemed useful to extend the simulations out any further. This means that for the later performed MD simulations of early interaction stages of NK-2 with the respective model lipid bilayers, it was not possible (in the opposite way) to start with the random coil conformation for NK-2 in the water phase and then to wait for the conversion in the well-defined secondary structure near the lipid surface to occur. It was instead decided to have the NK-2 approach the respective lipid surface already in the helix-hinge-helix structure expected near the surface.

NK-2 Membrane Association

As outlined at the end of the foregoing section, we started the simulation of the peptide–membrane association with an idealized helix-hinge-helix geometry of NK-2. Although experimental finding [10] and the consideration of polarizing effects (the peptide

Journal of PeptideScience

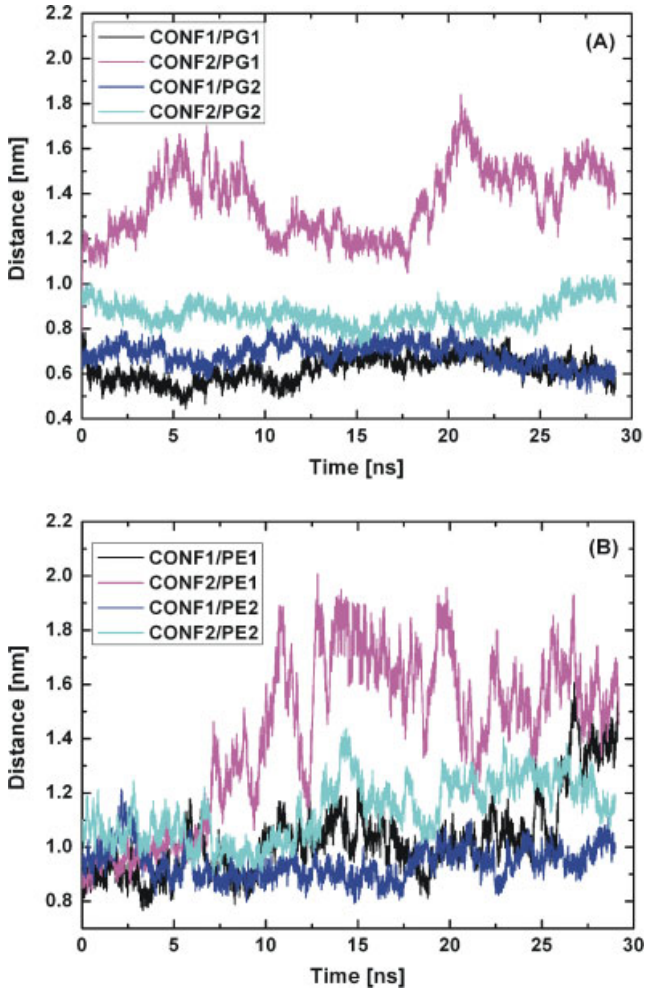

Figure 3. (A) Time series of the distance between the center of mass of NK-2 and the phosphorous atom of DPPG bilayer. (B) Similar plot for DPPE bilayer.

faces on the one side the extremely hydrophilic bulk water phase and on the other side the less hydrophilic head group region of the lipid bilayer) suggests that the approach near the lipid interface happens with the hydrophobic side of the peptide first, as a negative control, we also considered a second peptide orientation 'upside down' (cf. Methods). Only one peptide is attached to each leaflet of the bilayer. Moreover, the selected two peptide orientations in the model were considered reasonable to collect further (e.g. energetic, the role of amino residues in membrane association) arguments for this view. Considering the above described cutoff conditions, there are no direct interactions between the peptides to be expected. The initial configuration of NK-2/DPPG and NK-2/DPPE are shown in Figure 2(A) and (B), respectively.

Position and orientation of NK-2

The approach of NK-2 towards the model membrane surfaces, as shown via the *z*-component of the distance between the centre of mass of the peptide and the plane of the phosphorus atoms of the respective side of the lipid bilayer is displayed in Figure 3. In the PG1 (NK2/DPPG under NPAT conditions) system (Figure 3(A)), it is clearly visible that in the case of DPPG only the expected orientation, CONF1, with the hydrophobic side

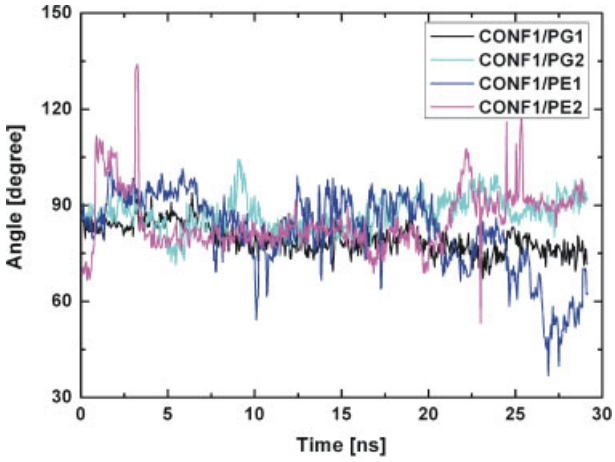

Figure 4. Angle formed by the helix of NK-2 (CONF1) with the membrane normal. The helix tilt angle is calculated by measuring the angle between the vertical *z* axis and the line formed by the atoms of residues Ile-10 and Lys-20. This shows that the more preferable orientation CONF1 peptide lies mostly parallel to the lipid/water interface.

of the peptide pointing towards the lipid interface leads to a strong interaction accompanied by partial insertion. The opposite orientation, CONF2, however, showed a tendency to detach from the lipid surface. Also in the PE1 (NK2/DPPE under NPAT conditions) system (Figure 3(B)), a stronger interaction between peptide and lipid bilayer is observed for the orientation case CONF1 (black line). The observed distances do however not indicate any real trend of insertion even for CONF1 which is consistent with neutron experiment data (Willumeit R, unpublished data). These results are also consistent with previous simulations showing that differences in the degree of peptide–lipid interaction were dependent on the starting orientation of the peptide [19,24]. For the respective systems simulated under NPγT conditions, PG2 (Figure 3(A)) and PE2 (Figure 3(B)), we observed a similar trend, namely, that the CONF1 situation leads to a closer approach of the peptide to the respective membrane surface than CONF2. Again, the peptide in CONF1 orientation shows stronger binding and deeper insertion into a PG than a PE membrane. This observation supports IRRAS and XR experimental results indicating that NK-2 does not adsorb to a condensed zwitterionic monolayer. In contrast, NK-2 adsorbs readily to anionic phospholipids and penetrates into both condensed and fluid anionic monolayers [15]. All simulated conditions showed an increase in total binding and subsequent penetration for the hydrophobically oriented peptides (CONF1), while the charge-oriented peptides (CONF2) appear to be at most located close to the charged membrane surface with no trace of penetration. The factors that contribute to a peptide binding to the membrane surface will be discussed in subsequent section.

To determine if the peptide is oriented parallel to the membrane surface, we calculated the angle formed by the helical fragment of the peptide with the membrane normal for the CONF1 orientation (Figure 4). The 90° represents a horizontal orientation relative to the membrane surface and 0 or 180° a vertical one. Although the secondary structure may change throughout the duration of the simulation, this region is assumed to form an α-helix. The omission of major secondary structure changes in the simulations is one cause of the fairly large fluctuations in the tilt angle. Nevertheless, we clearly found that CONF1 stays parallel to the membrane interface on both model membrane systems, consistent with the experimental surface IRRA spectra [14].

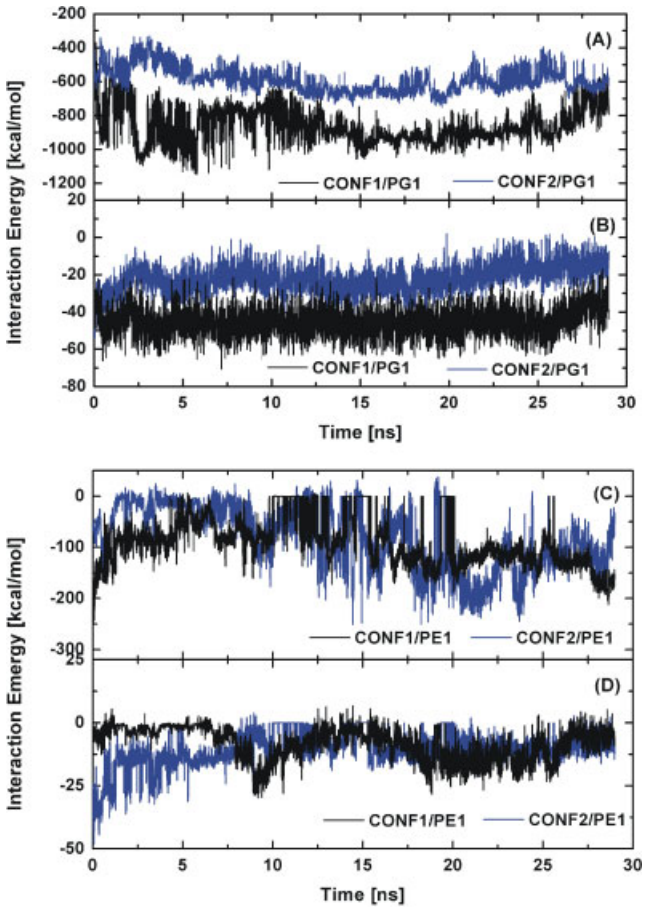

Figure 5. Association energy between NK-2 and model bilayer membranes. (A) Coulomb interaction energy in DPPG bilayer, (B) Lennard-Jones interaction energy in DPPG bilayer, (C) Coulomb interaction energy in DPPE bilayer and (D) Lennard-Jones interaction energy in DPPE bilayer.

However, one should have in mind that the peptides were placed relatively close to the respective membrane interface (cf. Figure 2(A) and (B)). In the more likely CONF1 case, the peptide attached quickly (within 1–2 ns) to the respective lipid surface undergoing only limited reorientation (cf. also Figure 3) and it remained closely attached to the lipid during the remaining simulation time. CONF2, on the other hand, showed a clear tendency to detach even more, than was initially set, from the respective membrane surface (Figure 3) with the remaining contacts being limited to the *N*-terminal region. During this process, a rotation of the CONF2 peptide about its long axis to nearly perpendicular orientation to the bilayer surface (data not shown) was observed. It is possible that, in much longer simulations starting with the peptides at a considerably greater distance from the bilayer interface, more pronounced rotations of the peptide helices about their long axes might occur. Although, we would expect that the final orientation of the peptide after the approach to the lipid surface in the CONF1 case would not change much, such longer simulations might allow a deeper understanding on the factors regulating the early stage of peptide–membrane association.

Interaction energy

Here, we present factors that are important for the observed NK-2 selectivity. As illustrated in Figure 5, showing both the electrostatic Coulomb and dispersion energy Lennard-Jones (LJ) contribution for the DPPG and DPPE bilayers, the NK-2 adsorption onto the respective membrane surface is mainly due to electrostatic interactions. Here, only the energy profile of models system simulated under NPAT is presented. The calculations indicate conclusively that CONF1 is the energetically clearly preferred configuration for membrane-association while the van der Waals and Columbic energy are considerably higher (less negative) for the CONF2 case. In addition, this result helps to explain the selectivity of NK-2 peptide towards the bacterial cell membrane composed mainly of phospholipid negatively charged phospholipids [61] and reference therein). In the following sections, we will only discuss results from the CONF1 case.

Table 2. Number of hydrogen bonds between peptide and lipids, between peptide and waters and between lipid and waters

	Glycerol head group	Phosphate oxygens	Waters
CONF1/PG1[a]	4.4 ± 0.6	18.7 ± 0.6	69.5 ± 1.9
Arg side chain[a]	0.2 ± 0.07	5.8 ± 0.3	13.9 ± 0.6
Lys side chain[a]	2.7 ± 0.6	11.8 ± 0.5	11.0 ± 0.9
Water[b]	1.6 ± 0.01	3.2 ± 0.05	–
CONF1/PE1[a]	–	5.4 ± 2.1	68.4 ± 2.8
Arg side chain[a]	–	1.9 ± 0.9	16.5 ± 1.4
Lys side chain[a]	–	1.6 ± 0.4	21.3 ± 1.8
Water[b]	–	2.7 ± 0.06	

[a] Hydrogen bond calculated per peptide.
[b] Hydrogen bond calculated per lipid.

Peptide–lipid contacts

To further characterize the intermolecular interaction of the peptide with the respective membrane surface, the number of hydrogen bonds (H-bonds) formed between peptide and lipid molecules were monitored. In this study, a hydrogen bond is assumed to exist when donor–acceptor distance is closer than 0.24 nm [62]. The occurrence hydrogen bond distribution between peptides and lipids is summarized in Table 2. The standard deviations are calculated by splitting the trajectory into five pieces (1-ns each) and then calculating the standard deviation from these pieces. Here, only the hydrogen bond formation calculated in the NPAT simulation, PG1 and PE1, is discussed.

Although at the end of the simulation time the peptide is embedded in the respective lipid head group regions to a different degree (more for DPPG than for DPPE), one can still expect a high concentration of hydrogen bond formation between peptide and water molecules in both cases as indicated by the values in the last column of the table. In the PG model, the positively charged amino acid side chains make the remaining hydrogen bonds predominantly with phosphate oxygen atoms of the PG head group while much less H-bonds are formed with the glycerol oxygen atoms. The observed high concentration of hydrogen bonds with the lipid head groups in the CONF1 case of DPPG can be explained in terms of preferable direct electrostatic interaction between the positively charged peptide amino acids and the negatively charged groups in the head group region of PG-lipids. This preferential direct electrostatic interaction starts when the peptide has reached a critical distance to the respective lipid.

By contrast, in the PE model, a lower concentration of hydrogen bonds is observed between NK2 and the head groups of this lipid.

Journal of PeptideScience

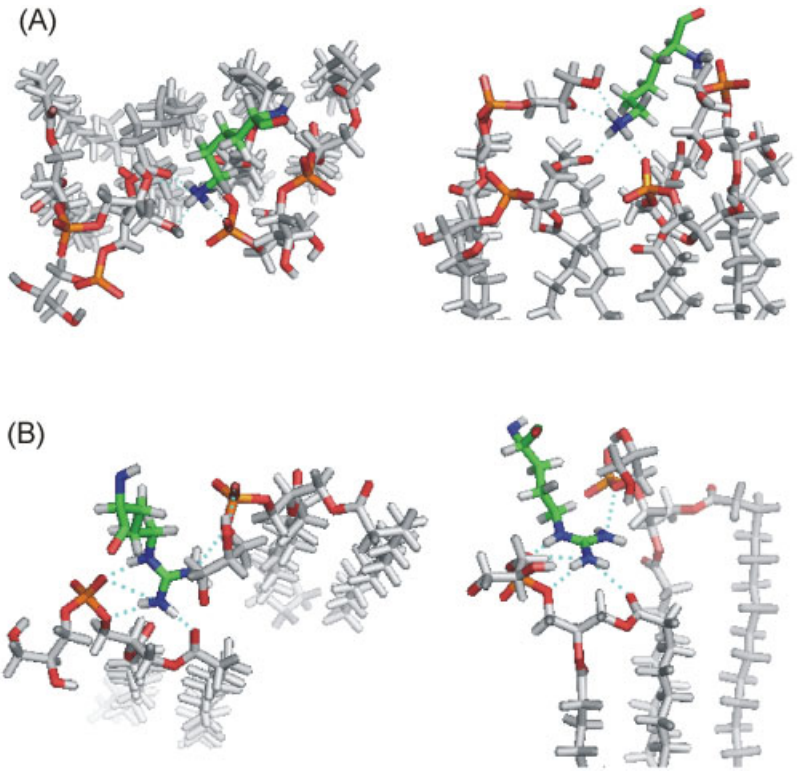

Figure 6. Binding of a lysine side chain (A) and arginine side chain (B) to three DPPG lipid molecules. Left: top view, right: side-view. The snapshot was taken from Lys1 and Arg4 residue, respectively. For peptide and lipids, the nitrogen atoms are shown in blue, oxygen in red and phosphorus in orange. For clarity, the carbon atoms of the arginine residue are shown in green, and the carbon atoms of the DPPG are shown in light grey.

This finding can be linked to the larger average distance between the peptide molecule and the DPPE head group region.

Figure 6 demonstrates, as a specific example for hydrogen bond formation, the ability of the guanidino nitrogen of the Arg4 and of the ammonium group of the Lys1 hydrogen-bonded to an adjacent DPPG head group. The snapshot is taken form the PG1 simulation. This finding is similar to a previous simulation study on the impact of the arginine containing AMP on the DPPC bilayer [23], suggesting the arginine side chain forms a complex hydrogen bond pattern with acyl ester oxygen (the oxygen of glycerol and the acyl chain) and with the phosphate of the PC head group. These findings suggest that the electrostatic/hydrogen bonding modulate the peptide–membrane affinity, which is stronger in the case of the charged DPPG bilayer than for the less charged DPPE bilayer.

To get further insight into the peptide–lipid interaction, we calculated radial distribution functions (RDFs) for each residue side chain with the phosphorus atoms of the respective lipid head group. The RDF provides a measure of the probability that an atom pair of a given type occurs at a certain distance, thus providing information about relative affinities between sets of atoms in the respective system. Figure 7 shows results (first peak which is at the same time the main peak) for radial distance distributions between the positively charged nitrogen atoms of the NK-2 amino acids (i.e. lysine and arginine) and the closest phosphorous atoms on the respective lipid bilayer head groups as averages over the last 5-ns of MD-production run. Note that, although, we modeled the peptide close to the membrane surface in both systems, the peptide shows different binding abilities to the different membrane surfaces. For the charged lipid DPPG (PG1 model, i.e. NPAT conditions, Figure 7(A)), the first peak for almost all charged amino acids appears close to 3.8 Å, indicating strong electrostatic interactions with the phosphate anions. These interactions of the charged amino acids along the helix chain cause the peptide to attach tightly to the DPPG membrane interface and eventually attribute to align its helical axis parallel to the interface. The CONF1 peptide behaves similar in the PG2 (i.e. NPγT conditions) model (data not shown), all positive charge amino acid residues lay close to the membrane phosphate moiety. These results further demonstrate the action of strong electrostatic forces against the initial polar interactions of the NK-2 with the bulk water and the lipid phases. They are the main reason for the observed strong trend of the whole peptide to partly insert (laterally) in the head group area of the DPPG bilayer.

Furthermore, to monitor the insertion of the amino acid residue into the membrane, we calculated the RDF between the nitrogen atoms of the charged amino acids of the peptide and the carboxyl oxygen atoms of the *sn*1 chains (cf. the labeling in Figure 12(A)) of the DPPG lipids. An observed pronounced peak at 2.8 Å reveals that the Lys1 and Arg4 side chains form hydrogen bonds with the mentioned carboxyl oxygen atoms (cf. Figure S2 as Supporting Information). In fact, the *sn*1 carboxyl groups are even slightly closer to the centre of the bilayer than the *sn*2 carboxyl groups. Therefore, a relatively deep insertion of those two residues into the membrane is assumed. This also indicates that the insertion of NK-2 into the bilayer membrane occurs via its *N*-terminus. In the DPPE model (PE1 model, Figure 7(B)), the Lys9, Arg16, Arg17 and Lys20 also showed a tendency to form electrostatic interaction with the phosphate groups as it was observed in DPPG model system. However, the quantitative effect is considerably weaker in DPPE than in DPPG (as e.g. indicated by the numeric values of g(r) and the number of amino acids involved showing a peak at about 3.8 Å). For CONF1 in the PE2

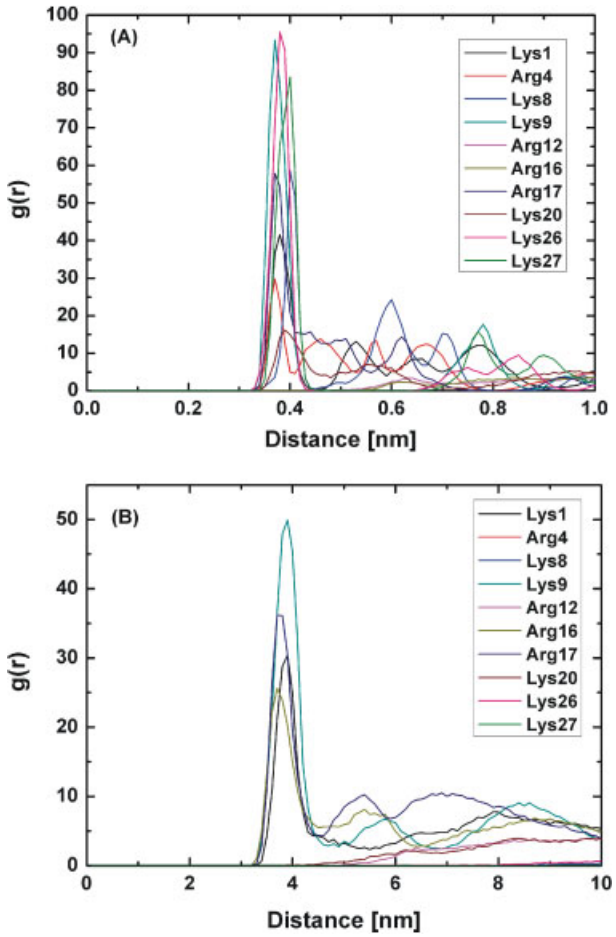

Figure 7. Radial distribution functions between the positively charged side chains of CONF1 and the phosphorus atoms of PG1 (A) and PE1 (B).

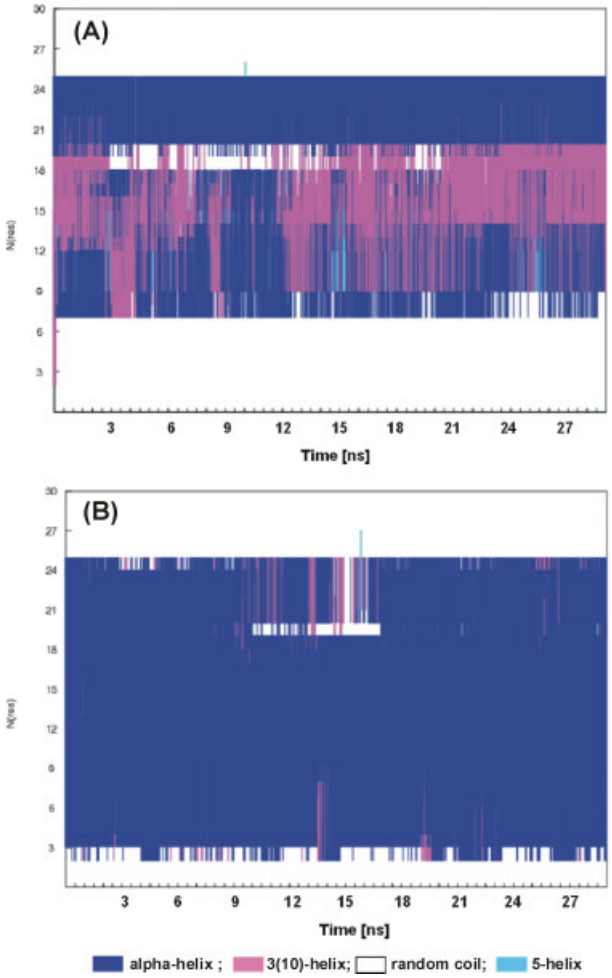

Figure 8. Secondary-structure profile of NK-2 (as determined by define secondary structure of proteins (DSSP) implemented in program SIMULAID). (A) CONF1 in DPPG bilayer. (B) CONF1 in DPPE. Blue portion of the plots represents the residues that have a helical conformation at a given time in the trajectory.

model system, a similar effect was also observed with a much smaller population of charge amino acid residues reside being close to the lipid phosphate group (data not shown). Our results indicate that the assumed bending region of the NK-2 helix-hinge-helix conformation, presented in the middle of the peptide sequence (Phe14), contributes to membrane association by the peptide in the present study. As such, it increased the propensity of the hydrophilic residues located on the hydrophobic face and promotes selective responses towards the anionic membrane. In addition, the partial insertion of hydrophobic residues, i.e. phenylalanine residues into the membrane (CONF1), mediates the primary binding to the cell membrane. This finding is likely to explain the existing data where the central hinge is responsible for the effective antibiotic activity of the AMPs with the helix-hinge-helix structure [63]. Summarizing, we can conclude that direct electrostatic interactions between positively charged amino acids of NK-2 and negatively charged groups at the membrane surface accelerate the peptide binding process while hydrophobic residues modulate the peptide insertion into membranes. These trends are further confirmed by the hydrogen bond formation between the peptide and the respective lipid.

Evolution of the NK-2 Conformation on Binding to Membranes

The concomitant secondary structure evolutions of the peptide in contact with both the anionic DPPG bilayer and the zwitterionic DPPE bilayer are shown in Figure 8. For both systems, we observed clearly distinct changes in secondary structure as also compared with the aqueous solution. Concerning the membrane-bound peptide, these data indicate a partial interruption of helical content of NK-2 in contact with DPPG from the typical $i \rightarrow i + 4(\alpha\text{-helix})$ situation to partial $i \rightarrow i + 3$ (3_{10}-helical) interaction, and to partial unstructured conformation. This result is obviously closely linked with the observed very strong interactions between the positively charged amino acid residues of NK-2 and the negatively charged phosphorous atoms in DPPG (cf. Section Interaction energy and Section Peptide-lipid contacts). To further investigate its flexibility, its phi and psi (ϕ, ψ) dihedral angles are plotted and compared with its starting structure (Figure 9). In the PG system, the structure of the assumed bending region of the peptide does not change due to the interaction with PG head groups. The backbone dihedral angles at the *N* and *C* terminal region actually show a deviation from an idealized helical (-60, -50) conformation. This is certainly a consequence of the strong electrostatic forces between the peptide and anionic membranes. In the presence of zwitterionic membranes, the peptide adopts mainly an α-helical structure and shows a disappearance of the bend structure. Since the peptide shows difference in the

Journal of PeptideScience

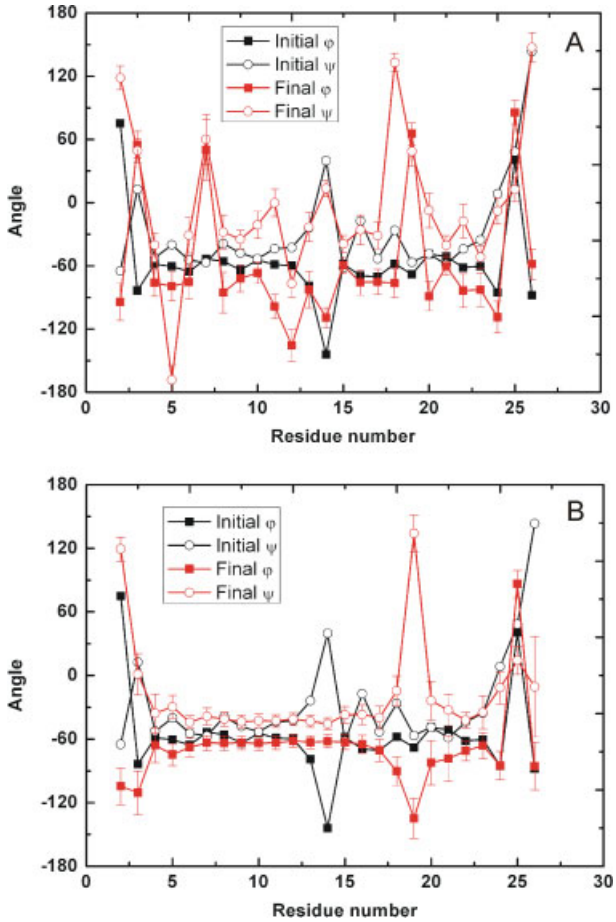

Figure 9. Dihedral angles of the CONF1 peptide in (A) PG1 (B) PE1.

secondary structure in different environments, these findings are therefore conceivable that a strong propensity of negatively charged PG to hydrogen bond to the positive charge residue of the peptide seems to correlate with loss of helicity. It is interesting to consider whether a more helical structure may be related to the low affinity to the membrane surface. As such, the segregation between hydrophobic and hydrophilic amino acids onto opposite sides of a helix is more pronounced, in turn, the hydrogen bond formation is considerably weaker in this conformation as seen in the RDF profile. This may reduce the ability of the intercalation and binding of peptide into the PE membrane surface. The influence of the environment on the mobility of the peptide structure is another parameter of our interest. Figure 10(A) shows the C_α position of the root mean square fluctuation (RMSF) of the individual residues, which measures their mobility. As can be seen, the RMSF of the peptide backbone is lowest in the DPPG system (black squares). It can be explained by the fact that the association with phospholipids significantly lowers the freedom of motion of the peptide residues, in turn, the conformation of the peptides is more restricted in the tightly bound state. In DPPE (light grey circle), higher fluctuations existed at the *N*- and *C*-terminal than in the middle of the peptide structure. This observation is confirmed by the RDF profile (Figure 7(B)), indicating that the charged amino acid residues in the middle of the chain, i.e. Lys 9, Arg 16, Arg 19 and Lys 20 are located close to the DPPE head group. Moreover, the peptide backbone for DPPE behaves comparable to that of peptide in water (grey triangle) systems. In addition, we observed a very high $C\alpha$ RMS deviation from the starting structure in PE and water simulations (see support information). This finding is indicating that the peptide is only weakly bound to the DPPE interface and mainly located in the water phase. This result is consistent with Specular X-ray reflectivity (XR) measurements [15], indicating no adsorption/penetration of NK-2 into condensed zwitterionic monolayers occurs at a physiological relevant lateral pressure of 30 mN/m. This is further confirmed by visualized clusters of conformations of a structure saved every 1-ns over the whole simulation time at different environmental conditions as shown in Figure 10. These configuration snapshots are colored-coded according to the simulation time step, the red color is for the starting structure and is then developing into the blue color for the final conformation. It is clearly seen that the peptide structure in the DPPG bilayer (Figure 10(B)) shows a considerably smaller conformational flexibility than in the DPPE bilayer case (Figure 10(C)) and water (Figure 10(D)), respectively. The simulations of NK-2 associated with the lipid membranes progressed towards an equilibrated structure during the first half of the simulations and showed structural stability than NK-2 in water, indicated by RMS deviation calculation (see Figure S1 in Supporting Information).

Influence on the Bilayer Structure

Electron density profile

Details of the locations of the peptide and the effect of peptide on the bilayer structure have also been analyzed using electron density profiles across the bilayer normal (*z*-axis) as shown in Figure 11. The comparison of the respective NK-2 electron density profiles (only CONF1 considered) for the two lipid bilayer systems only for DPPG (Figure 11(A)) shows a partial penetration of the peptide in the head group area while it stays more or less outside the DPPE interface (Figure 11(C)). As was demonstrated above, the overall orientation of the long axis of the peptide relative to the lipid interface is parallel for both cases. The corresponding diameter of the α-helix at the membrane interface is around 1.7 nm which can be well correlated with experimental findings [14,15]. In addition, we compared the positions of phosphate groups of the lipids that are close to the peptide (associating lipids) with those of the lipids that do not interact with the peptide (nonassociating lipids) in the same monolayer. Here, only monolayer in contact with CONF1 is considered. As such, we observed a slight reduction in bilayer thickness of DPPG (Figure 11(B)), while no clear profile change was detected in the DPPE bilayer (Figure 11(D)). The thinning of the membrane is consistent with the experimental observation of the interaction between the AMP LL-37 with the gel phase DPPG [32]. However, it is reported such interaction can induce an interdigitated phase (i.e. a slight partial overlap of the aliphatic tails of the upper and lower leaflets of lipid bilayers) in DPPG which we do not see. The situation in our models is however a bit different from the experiment, insofar as we have placed one peptide (in different orientation) on either site of the model bilayer. Although the mentioned change in the condensed DPPG bilayer thickness (cf. Figure 11(C)) is relatively small, it is comparable to SAXS experiment indicating a decrease in bilayer thickness of the liquid crystalline phase POPG about 2 Å [13]. Moreover, this finding concurs with SAXS that such no influence on PE membrane thickness. As already mentioned, we performed simulations under NPγT (PG2) conditions to avoid the artefact of a membrane thinning effect. We found only a slight change in the membrane thickness in this system (Figure 11(C) inset). This can

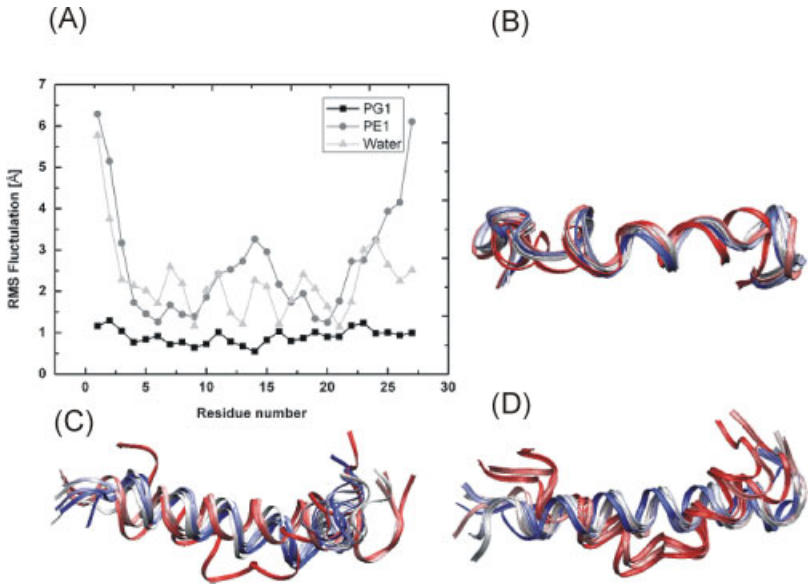

Figure 10. Average RMS fluctuations in MD simulation of NK-2 in water (light grey triangle) and with DPPG (black square) and with DPPE; grey circle) (A). The secondary structure evolution of NK-2, generated by clustering the whole trajectories of CONF1 in anionic DPPG lipid bilayers (B). CONF1 zwitteronic DPPE lipid bilayers(C) and NK-2 in water (D). Each conformation is color coded according to the saved structure (see text). Red tubes: NMR structure of NK-2. Blue tubes: the final conformation. The pictures were created with VMD [55].

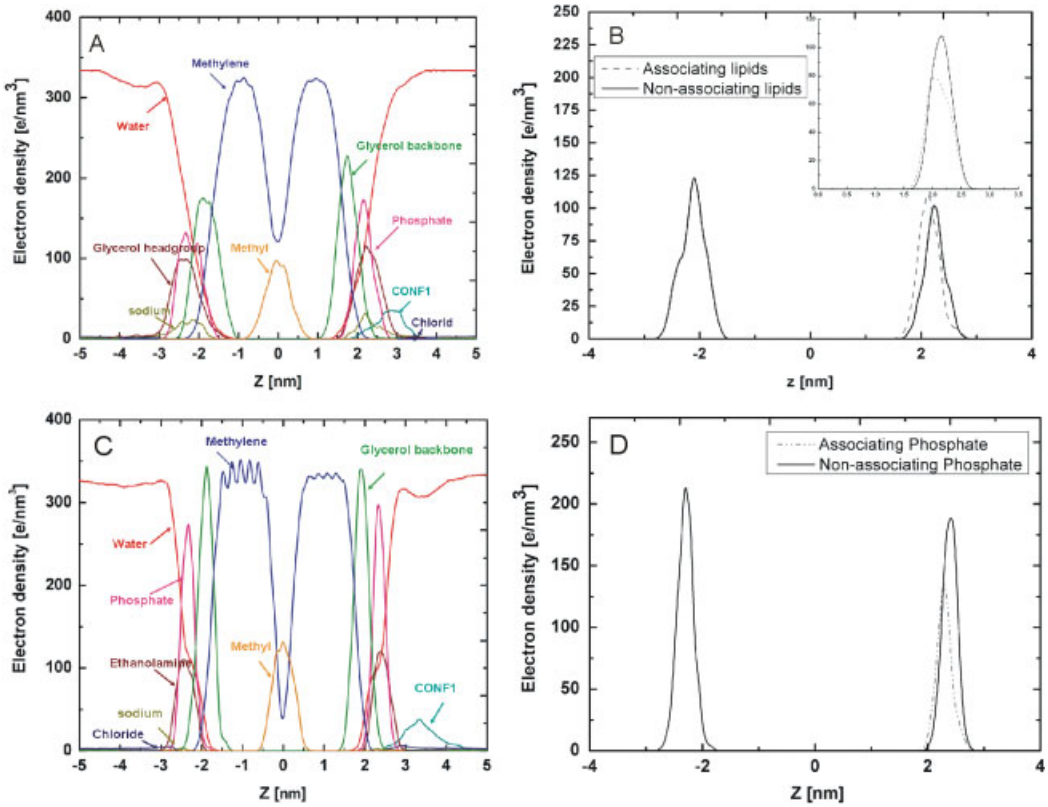

Figure 11. Averaged electron density profiles for various functional groups as a function of distance from the bilayer centre ($z = 0$). (A) PG1 system (B) PE1 system. (C) Highlight of the density profiles for the nonassociating phosphate group and for the associating phosphate group of DPPG in the PG1 system. The inset presents of that structure in the PG2 as comparison. The phosphate groups of the lipids that are within a distance of 1.5 nm of the peptide at any point during the simulation are labeled as associating phosphates. The other phosphates in the same leaflet are labeled as nonassociating phosphates. (D) The same distribution functions for PE1 system. Note that the right-hand side of electron density profile shows the distribution from the CONF1 – lipids association.

Journal of PeptideScience

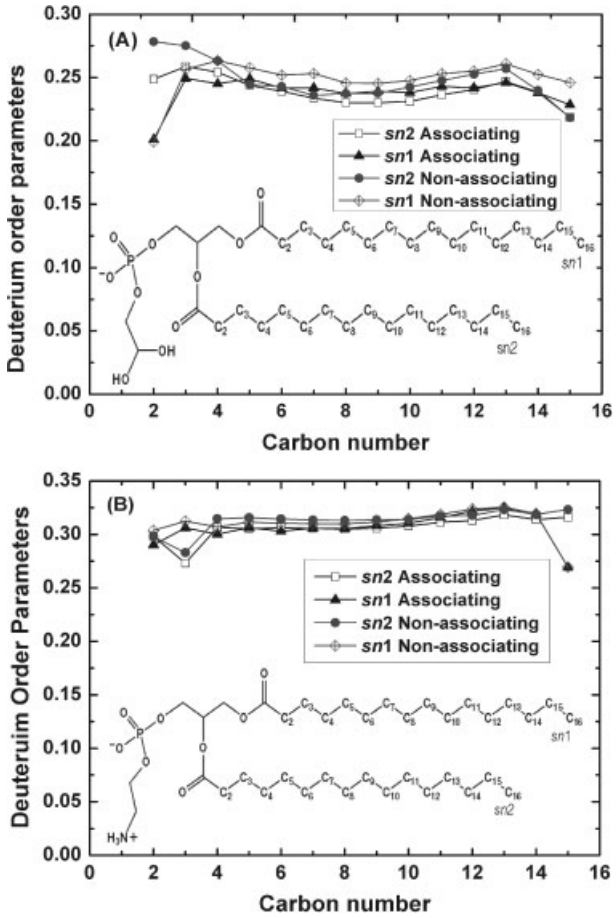

Figure 12. Order parameter profile for the lipid acyl chains of the peptide-associating and nonassociating (A) PG1 (B) PE1. The chemical structure of DPPG and DPPE is shown in the figure.

be explained by the fact that the peptide is not deeply inserted into the membrane whereby the lateral area was allowed to adjust during simulation. In the present study, an asymmetry of the electron density profile was observed for the methylene backbone in DPPE if one compares the left side (unrealistic CONF2) with the right (realistic CONF1) side. This is due to the higher mobility of the lipid head groups in DPPE for the CONF1 case (upper leaflet, right side in Figure 11(B)) than for the CONF2 situation (lower leaflet, left side in Figure 11(B)). This higher mobility is expected to cause the blurring of the sub-structure of the methylene profile in comparison to the CONF2 case.

Lipid order parameters

The average structure in the interior (aliphatic tails) of the bilayer was analyzed by calculating the deuterium order parameter, S_{CD}, using $S_{CD} = \frac{1}{2}\langle 3\cos^2\theta - 1\rangle$, where θ is the instantaneous angle between a vector along the methylene/methyl hydrogens of the acyl chain and the vector normal to the membrane plane, and the angular brackets indicate averaging over time-frames and over all lipids. Figure 12 shows the lipid order parameters profile for the associating and nonassociating lipids for DPPG and DPPE model membranes. The order parameter for the associating lipids in the NK2/DPPG system (Figure 12(A)) is slightly decreased at the methylene atoms close to the head group as compared with nonassociating lipids, indicating the peptide-induced disorder in the lipid acyl chains that are in close proximity to the binding site. This finding agrees with previous simulation on membrane-bound peptide [18,19,60,64]. Moreover, it is consistent with experiments that monitor the interaction of a peptide with the condense phase membrane, i.e. indolicidin [29] and PGLa [65]. This finding is contrary to our Fourier transform-infrared spectroscopy (FTIR) data, indicated that in the presence of the peptide, the dimyristoylphosphatidylglycerol (DMPG) membrane is stabilized, Tm is shifted to higher temperature and the rigidity of the acyl chains of DMPG increases in the fluid phase [13]. Here, one has of course to consider that the FTIR experiment characterizes the global structure of the membrane, whereas our simulation indicated a decrease in the order parameter only for the carbon atoms very close to the lipid head group, while no significant differences of the order parameter profile were observed for the rest of the aliphatic hydrocarbon chain. Here, FTIR is probably just not sensitive enough to register this relatively small local effect. It is not surprising that we did not notice a significant change in the middle of the chain as the peptide is not deeply inserted into its hydrophobic core. In the case of the DPPE bilayer (Figure 12(B)), there is no change in the overall order parameter on comparison between associating and nonassociating lipids as expected from the weak interaction with the peptide.

Conclusion

Computer modeling study combined with pre-existing experimental data elucidates the initial binding of the AMP NK-2 interaction to model membranes DPPG and DPPE. It was shown that the hydrophobic side of the peptide first approaches the lipid head group region. The interaction is then dominated by electrostatic forces. This behavior is related to the cell selectively of NK-2 to the bacterial cell membranes, whose lipid matrix consists mainly of PGs. The simulations support the assumption that the possible bend located in the middle of the helical structure plays an important role on membrane binding.

In the case of DPPG, the NK-2 is starting to insert in the head group region already during the limited available MD-simulation time, whereas for the zwitterionic DPPE, NK-2 is not deeply intercalating.

The hydrogen bond formation and electrostatic interaction between the cationic amino acids and the DPPG head groups help to hold the peptide close to the membrane surface. Moreover, the distribution of the charged amino acid residues along the helical axis causes the NK-2 peptide to be bound to the membrane surface more tightly. The insertion of hydrophobic residues induces a local membrane deformation resulting in a slight decrease in the acyl chain order parameters close to the head group and decreased membrane thickness.

An evaluation of the association of this peptide at higher concentration with various computational lipid membranes models and their capacity for membranes disruption is in the focus of our ongoing investigations.

In the present study, simulation under the NPAT and NPγT is carried out in parallel to avoid the artefact of the membrane thinning due to the confinement effect when the lipid bilayer begins to accommodate the peptide. Since we investigated at the condensed phase model system and the peptide is only adsorbed onto the membrane surface, the decrease of membrane thickness (local deformation) is expectedly more pronounced in the NPAT ensemble, where the area kept fixed during the period of

investigation. Besides that, both ensembles gave the similar trend in surface behavior and binding properties of NK-2 peptide at the membrane–water interface.

Acknowledgements

J. Pimthon acknowledges support from the Royal Thai Government. We would also like to thank Dr. Martin Siegert for help and technical support. We also thank Prof. Yiannis N. Kaznessis for the dipalmitoylphosphatidylglycerol topology file.

Supporting information

Supporting information may be found in the online version of this article.

References

1 Yeaman MR, Yount NY. Mechanisms of antimicrobial peptide action and resistance. *Pharmacol. Rev.* 2003; **55**: 27–55.
2 Zasloff M. Antimicrobial peptides of multicellular organisms. *Nature* 2002; **415**: 389–395.
3 Mookherjee N, Hancock RE. Cationic host defence peptides: innate immune regulatory peptides as a novel approach for treating infections. *Cell. Mol. Life. Sci.* 2007; **64**: 922–933.
4 Taheri-Araghi S, Ha B-Y. Physical basis for membrane-charge selectivity of cationic antimicrobial peptides. *Phys. Rev. Lett.* 2007; **98**: 168101–168104.
5 Brogden KA. Antimicrobial peptides: pore formers or metabolic inhibitors in bacteria? *Nat. Rev. Microbiol.* 2005; **3**: 238–250.
6 Palffy R, Gardlik R, Behuliak M, Kadasi L, Turna J, Celec P. On the physiology and pathophysiology of antimicrobial peptides. *Mol. Med.* 2009; **15**: 51–59.
7 Oren Z, Shai Y. Mode of action of linear amphipathic alpha-helical antimicrobial peptides. *Biopolymers* 1998; **47**: 451–463.
8 Andra J, Leippe M. Candidacidal activity of shortened synthetic analogs of amoebapores and NK-lysin. *Med. Microbiol. Immunol.* 1999; **188**: 117–124.
9 Liepinsh E, Andersson M, Ruysschaert JM, Otting G. Saposin fold revealed by the NMR structure of NK-lysin. *Nat. Struct. Biol.* 1997; **4**: 793–795.
10 Schroder-Borm H, Willumeit R, Brandenburg K, Andra J. Molecular basis for membrane selectivity of NK-2, a potent peptide antibiotic derived from NK-lysin. *Biochim. Biophys. Acta* 2003; **1612**: 164–171.
11 Andra J, Monreal D, Martinez de Tejada G, Olak C, Brezesinski G, Gomez SS, *et al*. Rationale for the design of shortened derivatives of the NK-lysin-derived antimicrobial peptide NK-2 with improved activity against Gram-negative pathogens. *J. Biol. Chem.* 2007; **282**: 14719–14728.
12 Schroder-Borm H, Bakalova R, Andra J. The NK-lysin derived peptide NK-2 preferentially kills cancer cells with increased surface levels of negatively charged phosphatidylserine. *FEBS Lett.* 2005; **579**: 6128–6134.
13 Willumeit R, Kumpugdee M, Funari SS, Lohner K, Navas BP, Brandenburg K, *et al*. Structural rearrangement of model membranes by the peptide antibiotic NK-2. *Biochim. Biophys. Acta* 2005; **1669**: 125–134.
14 Olak C, Muenter A, Andra J, Brezesinski G. Interfacial properties and structural analysis of the antimicrobial peptide NK-2. *J. Pept. Sci.* 2008; **14**: 510–517.
15 Olak C. *Biophysikalische Studien zur Wechselwirkung des antimikrobiellen Peptides NK-2 mit membran-mimetischen Systemen*. Doctoral Dissertation, Potsdam University, Potsdam, 2008.
16 Leontiadou H, Mark AE, Marrink SJ. Antimicrobial peptides in action. *J. Am. Chem. Soc.* 2006; **128**: 12156–12161.
17 Sengupta D, Leontiadou H, Mark A, Marrink S-J. Toroidal pores formed by antimicrobial peptides show significant disorder. *Biochim. Biophys. Acta* 2008; **1778**: 2308–2317.
18 Jang H, Ma B, Woolf TB, Nussinov R. Interaction of protegrin-1 with lipid lilayers: membrane thinning effect. *Biophys. J.* 2006; **91**: 2848–2859.
19 Fleming E, Maharaj NP, Chen JL, Nelson RB, Elmore DE. Effect of lipid composition on buforin II structure and membrane entry. *Proteins* 2008; **73**: 480–491.
20 Hsu JCY, Yip CM. Molecular dynamics simulations of indolicidin association with model lipid bilayers. *Biophys. J.* 2007; **92**: L100–L102.
21 Lensink MF, Christiaens B, Vandekerckhove J, Prochiantz A, Rosseneu M. Penetratin-membrane association: W48/R52/W56 shield the peptide from the aqueous phase. *Biophys. J.* 2005; **88**: 939–952.
22 Khandelia H, Kaznessis YN. Cation–π interactions stabilize the structure of the antimicrobial peptide indolicidin near membranes; molecular dynamics simulations. *J. Phys. Chem. B* 2007; **111**: 242–250.
23 Appelt C, Eisenmenger F, Kuhne R, Schmieder P, Söderhäll JA. Interaction of the antimicrobial peptide Cyclo(RRWWRF) with membranes by molecular dynamics simulations. *Biophys. J.* 2005; **89**: 2296–2306.
24 Polyansky AA, Volynsky PE, Arseniev AS, Efremov RG. Adaptation of a membrane-active peptide to heterogeneous environment. I. Structural plasticity of the peptide. *J. Phys. Chem. B* 2009; **113**: 1107–1119.
25 Lewis RN, Zweytick D, Pabst G, Lohner K, McElhaney RN. Calorimetric, x-ray diffraction, and spectroscopic studies of the thermotropic phase behavior and organization of tetramyristoyl cardiolipin membranes. *Biophys. J.* 2007; **92**: 3166–3177.
26 Latal A, Degovics G, Epand RF, Epand RM, Lohner K. Structural aspects of the interaction of peptidyl-glycylleucine-carboxyamide, a highly potent antimicrobial peptide from frog skin, with lipids. *Eur. J. Biochem.* 1997; **248**: 938–946.
27 Seto GW, Marwaha S, Kobewka DM, Lewis RN, Separovic F, McElhaney RN. Interactions of the Australian tree frog antimicrobial peptides aurein 1.2, citropin 1.1 and maculatin 1.1 with lipid model membranes: differential scanning calorimetric and Fourier transform infrared spectroscopic studies. *Biochim. Biophys. Acta* 2007; **1768**: 2787–2800.
28 Abrunhosa F, Faria S, Gomes P, Tomaz I, Pessoa JC, Andreu D, *et al*. Interaction and lipid-induced conformation of two cecropin-melittin hybrid peptides depend on peptide and membrane composition. *J. Phys. Chem. B* 2005; **109**: 17311–17319.
29 Shaw JE, Alattia JR, Verity JE, Prive GG, Yip CM. Mechanisms of antimicrobial peptide action: studies of indolicidin assembly at model membrane interfaces by *in situ* atomic force microscopy. *J. Struct. Biol.* 2006; **154**: 42–58.
30 van Kan EJM, Ganchev DN, Snel MME, Chupin V, van der Bent A, de Kruijff B. The peptide antibiotic clavanin A interacts strongly and specifically with lipid bilayers. *Biochemistry* 2003; **42**: 11366–11372.
31 Pott T, Dufourcq J, Dufourc EJ. Fluid or gel phase lipid bilayers to study peptide-membrane interactions? *Eur. Biophys. J.* 1996; **25**: 55–59.
32 Pabst G, Danner S, Karmakar S, Deutsch G, Raghunathan VA. On the propensity of phosphatidylglycerols to form interdigitated phases. *Biophys. J.* 2007; **93**: 513–525.
33 Sevcsik E, Pabst G, Jilek A, Lohner K. How lipids influence the mode of action of membrane-active peptides. *Biochim. Biophys. Acta* 2007; **1768**: 2586–2595.
34 Sevcsik E, Pabst G, Richter W, Danner S, Amenitsch H, Lohner K. Interaction of LL-37 with model membrane systems of different complexity: influence of the lipid matrix. *Biophys. J.* 2008; **94**: 4688–4699.
35 Pimthon J, Willumeit R, Lendlein A, Hofmann D. Computational modeling of anionic and zwitterionic lipid bilayers for investigating surface activities of bioactive molecules. *Mater. Res. Soc. Symp. Proc.* 2009; **1140**: 1140-HH09-07.
36 Neville F, Cahuzac M, Konovalov O, Ishitsuka Y, Lee KY, Kuzmenko I, *et al*. Lipid headgroup discrimination by antimicrobial peptide LL-37: insight into mechanism of action. *Biophys. J.* 2006; **90**: 1275–1287.
37 Gidalevitz D, Ishitsuka Y, Muresan AS, Konovalov O, Waring AJ, Lehrer RI, *et al*. Interaction of antimicrobial peptide protegrin with biomembranes. *Proc. Natl. Acad. Sci. U.S.A.* 2003; **100**: 6302–6307.
38 Brooks B, Bruccoleri R, Olafson B, States D, Swaminathan S, Karplus M. CHARMM: a program for macromolecular energy, minimization, and dynamics calculations. *J. Comput. Chem.* 1983; **4**: 187–217.
39 MacKerell AD, Bashford D, Bellott M, Dunbrack RL, Evanseck JD, Field MJ, *et al*. All-atom empirical potential for molecular modeling

Journal of PeptideScience

and dynamics studies of proteins. *J. Phys. Chem. B* 1998; **102**: 3586–3616.
40 Feig M, MacKerell AD Jr, Brooks CL III. Force field influence on the observation of π-helical protein structures in molecular dynamics simulations. *J. Phys. Chem. B* 2003; **107**: 2831–2836.
41 Feller SE, MacKerell AD. An improved empirical potential energy function for molecular simulations of phospholipids. *J. Phys. Chem. B* 2000; **104**: 7510–7515.
42 Durell SR, Brooks BR, Ben-Naim A. Solvent-induced forces between 2 hydrophillic groups. *J. Phys. Chem. B* 1994; **98**: 2198–2202.
43 Jorgensen WL, Chandrasekhar J, Madura JD, Impey RW, Klein ML. Comparison of simple potential functions for simulating liquid water. *J. Chem. Phys.* 1983; **79**: 926–935.
44 Ryckaert J-P, Ciccotti G, Berendsen H. Numerical integration of the cartesian equations of motion of a system with constraints: molecular dynamics of *n*-alkanes. *J. Comput. Phys.* 1977; **23**: 327–341.
45 Essmann U, Perera L, Berkowitz ML, Darden T, Lee H, Pedersen LG. A smooth particle mesh Ewald method. *J. Chem. Phys.* 1995; **103**: 8577–8593.
46 Zhang Y, Feller SE, Brooks BR, Pastor RW. Computer simulation of liquid/liquid interfaces. I. Theory and application to octane/water. *J. Chem. Phys.* 1995; **103**: 10252–10266.
47 Feller SE, Pastor RW. On simulating lipid bilayers with an applied surface tension: periodic boundary conditions and undulations. *Biophys. J.* 1996; **71**: 1350–1355.
48 Jensen MØ, Mouritsen OG, Peters GH. Simulations of a membrane-anchored peptide: structure, dynamics, and influence on bilayer properties. *Biophys. J.* 2004; **86**: 3556–3575.
49 Benz RW, Castro-Román F, Tobias DJ, White SH. Experimental validation of molecular dynamics simulations of lipid bilayers: a new approach. *Biophys. J.* 2005; **88**: 805–817.
50 Pimthon J, Willumeit R, Lendlein A, Hofmann D. All atom molecular dynamics simulation studies of fully hydrated gel phase DPPG and DPPE bilayers. *J. Mol. Struct.* 2009; **921**: 38–50.
51 Feller SE, Pastor RW. Constant surface tension simulations of lipid bilayers: the sensitivity of surface areas and compressibilities. *J. Chem. Phys.* 1999; **111**: 1281–1287.
52 Skibinsky A, Venable RM, Pastor RW. A molecular dynamics study of the response of lipid bilayers and monolayers to trehalose. *Biophys. J.* 2005; **89**: 4111–4121.
53 Jang H, Zheng J, Nussinov R. Models of beta-amyloid ion channels in the membrane suggest that channel formation in the bilayer is a dynamic process. *Biophys. J.* 2007; **93**: 1938–1949.
54 Feller SE, Zhang Y, Pastor RW, Brooks BR. Constant pressure molecular dynamics simulation: the Langevin piston method. *J. Chem. Phys.* 1995; **103**: 4613–4621.
55 Nose S, Klein ML. A study of solid and liquid carbon tetrafluoride using the constant pressure molecular-dynamics technique. *J. Chem. Phys.* 1983; **78**: 6928–6939.
56 Hoover WG. Canonical dynamics: equilibrium phase–space distributions. *Phys. Rev. A* 1985; **31**: 1695–1697.
57 Mezei M. Simulaid: a collection of utilities designed to help setting up molecular dynamics simulations. *J. Comput. Chem.* 1997; **18**: 812–815.
58 DeLano WL. *The PyMOL Molecular Graphics System*. Palo Alto, CA: DeLano Scientific; 2002.
59 Humphrey W, Dalke A, Schulten K. VMD: visual molecular dynamics. *J. Mol. Graph.* 1996; **14**: 33–38, 27–28.
60 Kandasamy SK, Larson RG. Binding and insertion of alpha-helical anti-microbial peptides in POPC bilayers studied by molecular dynamics simulations. *Chem. Phys. Lipids* 2004; **132**: 113–132.
61 Lohner K, Sevsik E, Pabst G. Liposome-based biomembrane mimetix systems: implications for lipid–peptide interactions. In *Advances in Planar Lipid Bilayers and Liposomes*, Leitmanova L (ed.). Elsevier: Amsterdam, 2008; 103–137.
62 De Loof H, Nilsson L, Rigler R. Molecular dynamics simulation of galanin in aqueous and nonaqueous solution. *J. Am. Chem. Soc.* 1992; **114**: 4028–4035.
63 Shin SY, Kang JH, Jang SY, Kim Y, Kim KL, Hahm KS. Effects of the hinge region of cecropin A(1–8)-magainin 2(1–12), a synthetic antimicrobial peptide, on liposomes, bacterial and tumor cells. *Biochim. Biophys. Acta* 2000; **1463**: 209–218.
64 Volynsky PE, Polyansky AA, Simakov NA, Arseniev AS, Efremov RG. Effect of lipid composition on the 'membrane response' induced by a fusion peptide. *Biochemistry* 2005; **44**: 14626–14637.
65 Pabst G, Grage S, Danner-Pongratz S, Jing W, Ulrich AS, Watts A, *et al*. Membrane thickening by the antimicrobial peptide PGLa. *Biophys. J.* 2008; **95**: 5779–5788.

